frontiers | Frontiers in Physics

TYPE Original Research
PUBLISHED 07 November 2022
DOI 10.3389/fphy.2022.1014900

OPEN ACCESS

EDITED BY
Zi-Lan Deng,
Jinan University, China

REVIEWED BY
Chujun Zhao,
Hunan University, China
Wenjun Liu,
Beijing University of Posts and Telecommunications (BUPT), China

*CORRESPONDENCE
Yingwei Wang,
wyw1988@csu.edu.cn
Jun He,
junhe@csu.edu.cn

SPECIALTY SECTION
This article was submitted to Optics and Photonics,
a section of the journal
Frontiers in Physics

RECEIVED 09 August 2022
ACCEPTED 19 October 2022
PUBLISHED 07 November 2022

CITATION
Wei H, Fan W, Dong Y, Wang Y, Zhou L, Wang Y and He J (2022), Black phosphorus quantum dots: Nonlinear optical modulation material with ultraviolet saturable absorption. *Front. Phys.* 10:1014900. doi: 10.3389/fphy.2022.1014900

Black phosphorus quantum dots: Nonlinear optical modulation material with ultraviolet saturable absorption

Hao Wei[1], Wenxuan Fan[1], Yulan Dong[2], Yiduo Wang[1], Li Zhou[1], Yingwei Wang[1]* and Jun He[1]*

[1]Hunan Key Laboratory of Nanophotonics and Devices, School of Physics and Electronics, Central South University, Changsha, China, [2]Key Laboratory of Hunan Province for Statistical Learning and Intelligent Computation, School of Mathematics and Statistics, Hunan University of Technology and Business, Changsha, China

Black phosphorus has attracted great interest for optical modulation and optoelectronic devices because of its ultrathin layer structure, tunable band gap, and high in-plane anisotropy. In particular, in the near-infrared and mid-infrared bands, proof-of-concept applications, including saturable absorber resonators, photodetectors, and optical modulators based on 2D black phosphorus nanosheets, have been reported one after another. However, relatively few studies about black phosphorus have been reported in the ultraviolet band. Moreover, the poor stability of black phosphorus has also limited its development in practical applications. Here, we successfully prepared ultra-small black phosphorus quantum dots (BPQDs) with an average thickness of 2.0 $\pm$ 0.4 nm and a diameter of 2.2 $\pm$ 0.6 nm. Furthermore, we also fabricated BPQD-Ormosil gel glasses. Through an open-aperture Z-scan experiment, BPQD-Ormosil gel glasses demonstrated excellent nonlinear optical modulation in the ultraviolet band, which proposes a new idea for ultraviolet optical modulation elements such as saturable absorption devices.

KEYWORDS

nonlinear optics, black phosphorus quantum dots (BPQDs), BPQD-Ormosil gel glasses, ultraviolet saturable absorption, optical modulation

Introduction

Black phosphorus (BP) nanomaterials possess extraordinary properties, including high carrier mobility [1], layer-dependent bandgap [2], and anisotropic in-plane lattice structure [3]. Using these excellent physical and chemical properties of BP, researchers have realized proof-of-concept applications of BP field-effect transistors with atomic layer thickness [1], photodetectors [4], electro-optic polarization modulators [5], saturable absorbers [6], and others [7–10]. Considering its optical modulation ability, the direct band gap of BP nanosheets is adjustable from 0.3 to 2.0 eV with the number of layers, enabling broadband optical modulation from the visible to the mid-infrared region [11, 12]. It is noteworthy that because BP is free from dangling bonds on the surface, it is

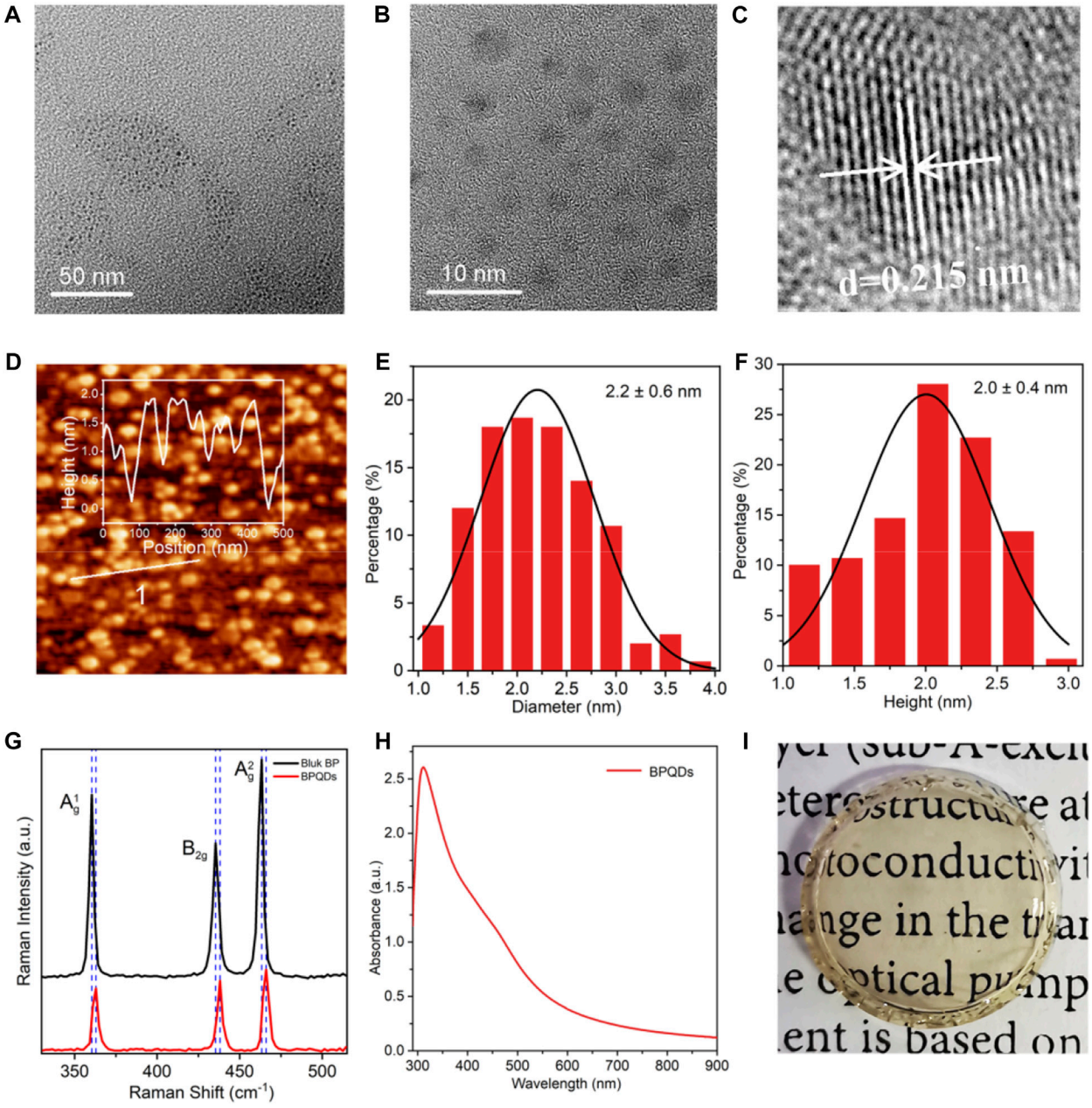

FIGURE. 1
Characterizations of BPQDs and BPQD-Ormosil gel glasses. **(A,B)** TEM and magnified TEM images of BPQDs. **(C)** High-resolution TEM images. **(D)** AFM images of BPQDs. Inset: height profile corresponding to line 1 in Figure 1 **(D)**. **(E)** Statistical analysis of the diameter of BPQDs determined by TEM. **(F)** Statistical analysis of BPQD height measured by AFM. **(G)** Raman spectra. **(H)** UV-vis absorption spectrum of the BPQDs. **(I)** Optical photograph of the BPQD-Ormosil gel glasses.

compatible with the Si substrate and can be integrated very well. BP is featured as an ideal candidate for an on-chip two-dimensional (2D) optical modulator, enabling new applications of 2D material photonic [13] devices.

By engineering morphology, the BP nanobelts [14, 15] and zero-dimensional QDs [16] with unique features can be obtained due to edge states and quantum confinement effects. BP QDs were derived from the 2D BP nanosheets by ultrasonic liquid phase exfoliation, solvothermal treatment approaches, and electrochemical exfoliation [16–19]. Conventional 2D materials, such as graphene and transition metal compounds of carbon or nitrogen, always

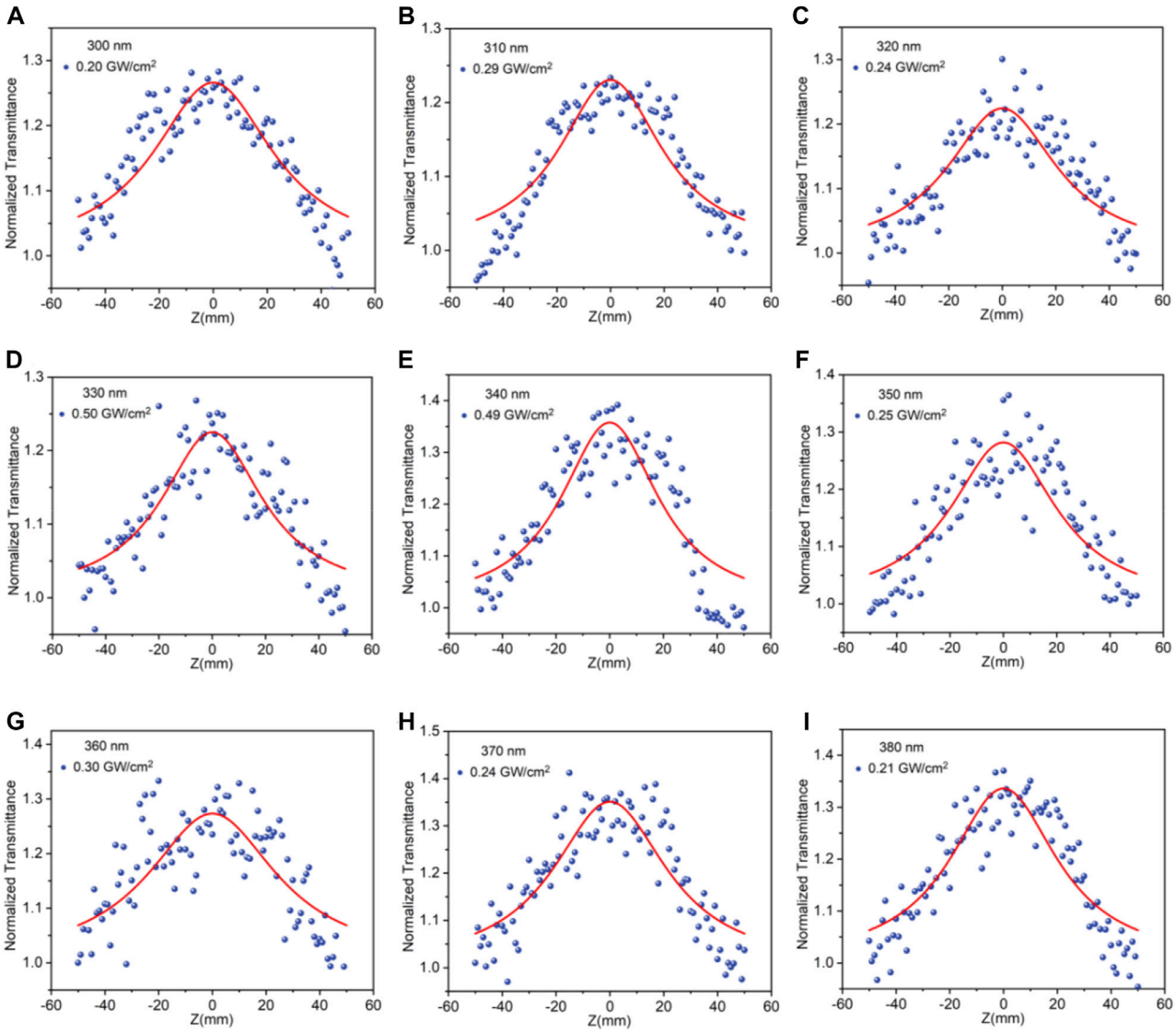

FIGURE 2
OA Z-scan results of BPQD-Ormosil gel glasses at excitation intensities of different ultraviolet wavelengths. **(A–I)**: 300, 310, 320, 330, 340, 350, 360, 370, and 380 nm.

show characteristics like atomically thin thicknesses and unique chemical and physical properties different from their bulk [20, 21]. BPQDs have ultrasmall sizes, wide tunable band gaps, great edge states, and higher surface-to-volume ratios [16]. Based on these favorable properties, BPQDs have been extensively investigated in broad fields like optoelectronics [17], biomedicine [22], bioimaging [23], and photovoltaics [24], to mention a few. Moreover, tremendous efforts have been devoted to optical modulation applications such as all-optical and saturable absorbers for ultrashort pulsed laser generation [25]. Ultrashort pulsed generation based on semiconductor saturable absorber mirrors has been around for half a century. Diverse 2D materials show an expected saturable absorption response in broadband [26–28]. In recent years, semiconductor saturable absorber resonators based on graphene [29], transition metal dichalcogenides [30–32], BP [33, 34], and other low-dimensional materials [35–38] have been reported in the near-infrared and mid-infrared regions. Due to the limitation to nonlinear saturable absorber materials, the wavelength of the ultrashort pulsed laser is mainly limited in the range of 0.8–2.0 μm. Obtaining materials with excellent optical modulation properties, such as saturable absorption properties in visible wavelength and especially in ultraviolet

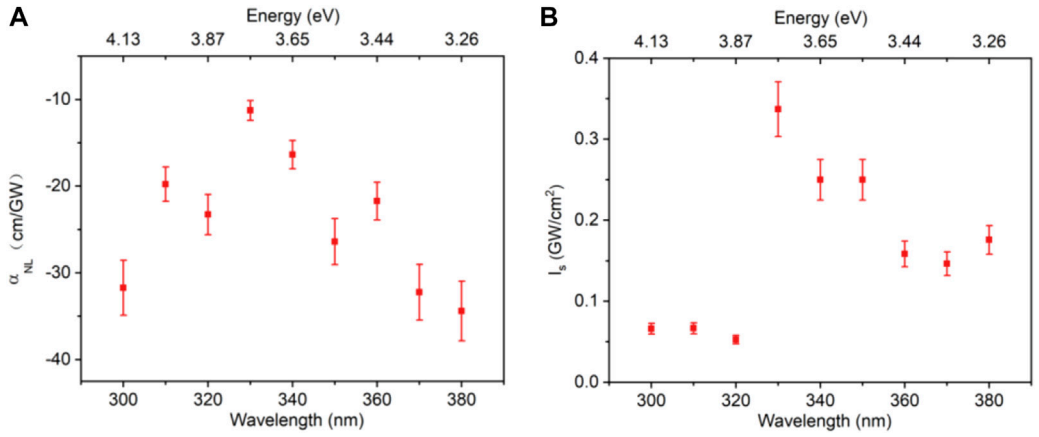

FIGURE 3
Analysis of nonlinear optical parameters of BPQD-Ormosil gel glasses. **(A)** Nonlinear absorption coefficient with error bars and **(B)** comparison of the saturable absorption intensity with error bars.

wavelength range, is an effective way to break through the wavelength limitation mentioned earlier. To address this issue, 2D material saturable absorbers were explored to realize pulsed lasers in the visible spectral range recently [39]. However, the short ultraviolet wavelength laser generation *via* direct methods is still a big challenge because of the lack of suitable ultraviolet saturable absorber materials.

In this work, we successfully prepared ultra-small BPQDs with an average thickness of 2.0 ± 0.4 nm and a diameter of 2.2 ± 0.6 nm by liquid-phase exfoliation. In order to avoid the degradation of QDs, BPQD-Ormosil gel glasses were fabricated. Furthermore, through an open-aperture (OA) Z-scan experiment, we demonstrated that BPQD-Ormosil gel glasses show excellent saturable absorption response in the ultraviolet region, opening a new promising application for optical modulation in the ultraviolet region.

Results and discussion

The liquid-phase exfoliation approach was used to prepare ultrasmall BPQDs. First, BP powder was added to the N-methyl-2-pyrrolidone (NMP) solution. The solution was placed in a mortar and thoroughly pounded using a pestle. Then, it was exfoliated by using an ultrasonic disruptor for 8 h in an ice bath. The resulting solution then underwent gradient centrifugation. The precipitate obtained from centrifugation at 18,000 rpm was the prepared BPQDs used in this work.

The typical sol-gel method [40] was used to fabricate BPQD-Ormosil gel glasses. Tetraethoxysilane ($Si(OC_2H_5)_4$, TEOS, 8.0 ml), 3-glycidoxypropyl-trimethoxysilane ($CH_2OCHCH_2O(CH_2)_3Si(OCH_3)_3$, GPTMS, 3.5 ml), H_2O (3.7 ml), and ethanol (12.1 ml) were mixed together with continuous magnetic stirring. A little amount of hydrochloric acid (HF) was added to make the pH of the solution equal to 2. With 2 h stirring of the mixture, the proper amount of 3-aminopropyltriethoxysilane ($NH_2(CH_2)_3Si(OC_2H_5)_3$, APTES) was added to neutralize the mixture pH and make it equal to 7. Then, the mixture of 9 ml of the DMF solution and synthesized BPQDs was gradually added. The mixed solution was continuously stirred for 15 mins. Next, the solution was cast onto individual polystyrene cells. Afterward, it was put in a dry environment to age and dry naturally.

The characterizations of BPQDs and BPQD-Ormosil gel glasses are shown in Figure 1. Figures 1A–C depict the morphological images of BPQDs acquired by transmission electron microscopy (TEM). The characterizations shown in Figures 1A,B exhibit morphology of the ultrasmall size BPQDs with uniform distribution. In Figure 1C, the high-resolution TEM image shows the 0.215 nm spacing between lattice fringes corresponding to the (014) plane of the BP. Figure 1D shows the atomic force microscopic (AFM) image of BPQDs, confirming the nanoscale thickness of prepared BPQDs. As per the statistical analyses shown in Figures 1E and F, the average diameter of BPQDs is 2.2 ± 0.6 nm and the mean thickness of BPQDs is 2.0 ± 0.4 nm. Figure 1G shows the Raman spectra of BPQDs with three typical Raman peaks corresponding to the A_g^1, B_{2g}, and A_g^2 vibrational modes, respectively. Relative to the bulk BP, Raman peaks of BPQDs show a blue shift, suggesting that the average thickness of BPQDs is thinner than bulk BP, according to a previous report [17]. Figure 1H shows the absorption spectra of BPQDs, suggesting a considerable absorption in the visible

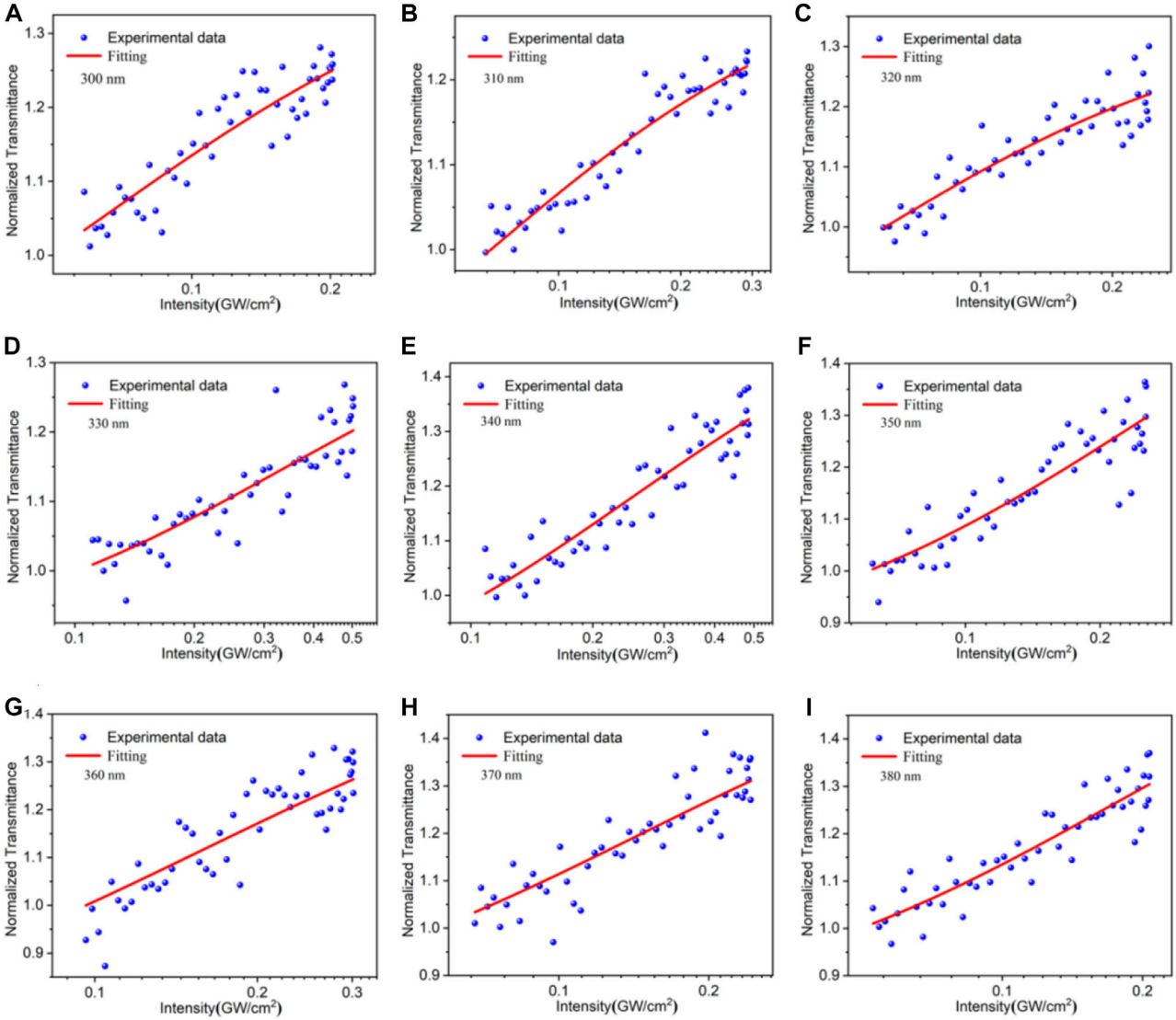

FIGURE 4
Fitting results of the saturable absorption intensity at different wavelengths. **(A–I)**: 300, 310, 320, 330, 340, 350, 360, 370, and 380 nm.

and ultraviolet regions. Figure 1 (I) shows the optical photograph of the prepared BPQD-Ormosil gel glasses, in which the thickness of the BPQD-Ormosil gel glasses is about 1 mm and the diameter is about 1.5 cm.

In order to research the nonlinear optical response of BPQDs, we conducted the OA Z-scan experiment. More details on the OA Z-scan experiment can be found in the previous report [26]. In the experiment, the incident laser is a mode-locked femtosecond pulsed laser with a repetition frequency of 2 kHz and a pulse width of 35 fs. The femtosecond laser with 800 nm wavelength can output a specific wavelength by using the optical parametric amplifier. The beam splitter splits the main beam into two beams to be used in the OA Z-scan experiment. One beam is defined as the reference beam to eliminate the experimental error. The excitation beam is incident on the sample, and its transmittance is recorded by using the power meter.

Figures 2A–I show the OA Z-scan results of BPQD-Ormosil gel glasses at ultraviolet wavelengths 300, 310, 320, 330, 340, 350, 360, 370, and 380 nm at different light intensities. As shown in Figure 2, BPQD-Ormosil gel glasses exhibit typical saturable absorption (SA) response at the ultraviolet wavelength range from 300 to 380 nm. Furthermore, we extracted nonlinear optical parameters of BPQD-Ormosil gel glasses, including the nonlinear absorption coefficient α_{NL} and saturable absorption

intensity I_s. According to the relevant theory [41], the data in Figure 2 can be fitted by the following equation:

$$T = 1/[sqrt\pi q_0] \int_{-\infty}^{+\infty} ln\ [1 + q_0\, exp(-x^2)]dx, \quad (1)$$

where T is the normalized transmittance, $q_0 = \beta q I_0 L_{eff}$, $L_{eff} = (1 - e^{-\alpha_0 L})/\alpha_0$ is the effective thickness of the sample, I_0 is the peak intensity of the incident laser, and L is the actual thickness of the sample. Figure 3A summarizes the extracted nonlinear absorption coefficients.

The saturable absorption intensities I_s can be fitted by the following equation (25):

$$T = 1 - A_s/(1 + I/I_s) - A_{ns}, \quad (2)$$

where A_{ns} is the non-saturable component and A_s is the modulation depth. As shown in Figure 4, the fitting results of the saturation intensity range from 0.05 to 0.35 GW/cm^2.

Figure 3 shows the nonlinear optical parameters of BPQD-Ormosil gel glasses at different wavelengths, including α_{NL} and I_s. All error bars were less than 10%, showing that the experiments are repeatable. The nonlinear absorption coefficient shows wavelength-dependent characteristics. As the wavelength changes from 310 nm to 380 nm, the maximum value of the nonlinear absorption coefficient occurs at the 330 nm wavelength. It may attribute to a strong light–matter interaction near 330 nm wavelength, which can be observed in the linear optical absorption spectrum in Figure 1H. The comparatively maximum value of the nonlinear absorption coefficient appears at 330 nm, considering the saturable absorption intensity as a function of excitation wavelength. When the photon energy is large enough, saturable absorption is no longer dominant, but there is more energy loss in the form of collisions. Interestingly, the saturable absorption intensity of BPQDs is as low as 0.05 GW/cm^2 near the 300 nm wavelength, which would benefit the stability of the ultrashort pulse generation system. Overall, these results indicate the promising potential of BPQD-Ormosil gel glasses for ultraviolet saturable absorption optical modulation devices.

Conclusion

We successfully prepared ultra-small black phosphorus quantum dots (BPQDs) with an average thickness of 2.0 ± 0.4 nm and a diameter of 2.2 ± 0.6 nm. Moreover, BPQD-Ormosil gel glasses were prepared to improve their stability in ambient conditions. The BPQD-Ormosil gel glasses demonstrated an interesting saturable absorption response in the ultraviolet region. Meanwhile, the wavelength-dependent nonlinear absorption coefficient and low saturable absorption intensity were observed. Our results enrich the ultraviolet light manipulation material family and provide a new idea for ultraviolet optical modulation, such as a saturable absorber.

Data availability statement

The original contributions presented in the study are included in the article/Supplementary Material; further inquiries can be directed to the corresponding authors.

Author contributions

YW and JH conceived the idea. HW and WF performed the experiments. YD, YW, and LZ conducted the characterization of nanostructures. The manuscript was written through the contributions of all authors. All authors have approved the final version of the manuscript.

Funding

The authors are grateful for the financial support from the National Natural Science Foundation of China (Nos. 61,874141 and 11904239), the Natural Science Foundation of Hunan Province (Grant Nos. 2021JJ40709 and 2022JJ20080), and the Open Sharing Fund for Large-scale Instruments and Equipment of Central South University.

Conflict of interest

The authors declare that the research was conducted in the absence of any commercial or financial relationships that could be construed as a potential conflict of interest.

Publisher's note

References

1. Li L, Yu Y, Ye GJ, Ge Q, Ou X, Wu H, et al. Black phosphorus field-effect transistors. *Nat Nanotechnol* (2014) 9:372–7. doi:10.1038/nnano.2014.35

2. Ling X, Wang H, Huang S, Xia F, Dresselhaus MS. The renaissance of black phosphorus. *Proc Natl Acad Sci U S A* (2015) 112:4523–30. doi:10.1073/pnas.1416581112

3. Xia F, Wang H, Jia Y. Rediscovering black phosphorus as an anisotropic layered material for optoelectronics and electronics. *Nat Commun* (2014) 5:4458. doi:10.1038/ncomms5458

4. Guo Q, Pospischil A, Bhuiyan M, Jiang H, Tian H, Farmer D, et al. Black phosphorus mid-infrared photodetectors with high gain. *Nano Lett* (2016) 16:4648–55. doi:10.1021/acs.nanolett.6b01977

5. Biswas S, Grajower MY, Watanabe K, Taniguchi T, Atwater HA. Broadband electro-optic polarization conversion with atomically thin black phosphorus. *Science* (2021) 374:448–53. doi:10.1126/science.abj7053

6. Zhang M, Wu Q, Zhang F, Chen L, Jin X, Hu Y, et al. 2D black phosphorus saturable absorbers for ultrafast photonics. *Adv Opt Mater* (2019) 7:1800224. doi:10.1002/adom.201800224

7. Dai J, Zeng XC. Bilayer phosphorene: Effect of stacking order on bandgap and its potential applications in thin-film solar cells. *J Phys Chem Lett* (2014) 5:1289–93. doi:10.1021/jz500409m

8. Deng Y, Luo Z, Conrad NJ, Liu H, Gong Y, Najmaei S, et al. Black phosphorus–monolayer MoS_2 van der Waals heterojunction p–n diode. *ACS Nano* (2014) 8:8292–9. doi:10.1021/nn5027388

9. Kou L, Frauenheim T, Chen C. Phosphorene as a superior gas sensor: Selective adsorption and distinct I–V response. *J Phys Chem Lett* (2014) 5:2675–81. doi:10.1021/jz501188k

10. Fei R, Faghaninia A, Soklaski R, Yan J-A, Lo C, Yang L. Enhanced thermoelectric efficiency via orthogonal electrical and thermal conductances in phosphorene. *Nano Lett* (2014) 14:6393–9. doi:10.1021/nl502865s

11. Zhang G, Huang S, Chaves A, Song C, Özçelik VO, Low T, et al. Infrared fingerprints of few-layer black phosphorus. *Nat Commun* (2017) 8:14071. doi:10.1038/ncomms14071

12. Peng R, Khaliji K, Youngblood N, Grassi R, Low T, Li M. Midinfrared electro-optic modulation in few-layer black phosphorus. *Nano Lett* (2017) 17:6315–20. doi:10.1021/acs.nanolett.7b03050

13. Huang L, Ang K-W. Black phosphorus photonics toward on-chip applications. *Appl Phys Rev* (2020) 7:031302. doi:10.1063/5.0005641

14. Li J, Gao Z, Ke X, Lv Y, Zhang H, Chen W, et al. Growth of black phosphorus nanobelts and microbelts. *Small* (2018) 14:1702501. doi:10.1002/smll.201702501

15. Liu Z, Sun Y, Cao H, Xie D, Li W, Wang J, et al. Unzipping of black phosphorus to form zigzag-phosphorene nanobelts. *Nat Commun* (2020) 11:3917. doi:10.1038/s41467-020-17622-6

16. Gui R, Jin H, Wang Z, Li J. Black phosphorus quantum dots: Synthesis, properties, functionalized modification and applications. *Chem Soc Rev* (2018) 47:6795–823. doi:10.1039/C8CS00387D

17. Zhang X, Xie H, Liu Z, Tan C, Luo Z, Li H, et al. Black phosphorus quantum dots. *Angew Chem Int Ed* (2015) 54:3653–7. doi:10.1002/anie.201409400

18. Mayorga-Martinez CC, Mohamad Latiff N, Eng AYS, Sofer Z, Pumera M. Black phosphorus nanoparticle labels for immunoassays via hydrogen evolution reaction mediation. *Anal Chem* (2016) 88:10074–9. doi:10.1021/acs.analchem.6b02422

19. Gu W, Pei X, Cheng Y, Zhang C, Zhang J, Yan Y, et al. Black phosphorus quantum dots as the ratiometric fluorescence probe for trace mercury ion detection based on inner filter effect. *ACS Sens* (2017) 2:576–82. doi:10.1021/acssensors.7b00102

20. Chen K-F, Cai P, Peng H-L, Xue X-G, Wang Z-M, Sun L-X. $Ti_3C_2T_x$ MXene for organic/perovskite optoelectronic devices. *J Cent South Univ* (2021) 28:3935–58. doi:10.1007/s11771-021-4846-z

21. Jiang H-H, Su H, Chen L-X, Tan X-W. GO-induced effective interconnection layer for all solution-processed tandem quantum dot light-emitting diodes. *J Cent South Univ* (2021) 28:3737–46. doi:10.1007/s11771-021-4850-3

22. Li Y, Liu Z, Hou Y, Yang G, Fei X, Zhao H, et al. Multifunctional nanoplatform based on black phosphorus quantum dots for bioimaging and photodynamic/photothermal synergistic cancer therapy. *ACS Appl Mater Inter* (2017) 9:25098–106. doi:10.1021/acsami.7b05824

23. Lee HU, Park SY, Lee SC, Choi S, Seo S, Kim H, et al. Black phosphorus (BP) nanodots for potential biomedical applications. *Small* (2016) 12:214–9. doi:10.1002/smll.201502756

24. Chen W, Li K, Wang Y, Feng X, Liao Z, Su Q, et al. Black phosphorus quantum dots for hole extraction of typical planar hybrid perovskite solar cells. *J Phys Chem Lett* (2017) 8:591–8. doi:10.1021/acs.jpclett.6b02843

25. Xu Y, Wang Z, Guo Z, Huang H, Xiao Q, Zhang H, et al. Solvothermal synthesis and ultrafast photonics of black phosphorus quantum dots. *Adv Opt Mater* (2016) 4:1223–9. doi:10.1002/adom.201600214

26. Wang Y, Wang Y, Chen K, Qi K, Xue T, Zhang H, et al. Niobium carbide MXenes with broad-band nonlinear optical response and ultrafast carrier dynamics. *ACS Nano* (2020) 14:10492–502. doi:10.1021/acsnano.0c04390

27. Wang Y, Mu H, Li X, Yuan J, Chen J, Xiao S, et al. Observation of large nonlinear responses in a graphene-Bi_2Te_3 heterostructure at a telecommunication wavelength. *Appl Phys Lett* (2016) 108:221901. doi:10.1063/1.4953072

28. Wei H, Wang Y, Wang Y, Fan W, Zhou L, Long M, et al. Giant two-photon absorption in MXene quantum dots. *Opt Express* (2022) 30:8482–93. doi:10.1364/OE.450617

29. Bao Q, Zhang H, Wang Y, Ni Z, Yan Y, Shen ZX, et al. Atomic-layer graphene as a saturable absorber for ultrafast pulsed lasers. *Adv Funct Mater* (2009) 19:3077–83. doi:10.1002/adfm.200901007

30. Chen B, Zhang X, Wu K, Wang H, Wang J, Chen J. Q-switched fiber laser based on transition metal dichalcogenides MoS_2, $MoSe_2$, WS_2, and WSe_2. *Opt Express* (2015) 23:26723–37. doi:10.1364/OE.23.026723

31. Li L, Pang L, Wang R, Zhang X, Hui Z, Han D, et al. Ternary transition metal dichalcogenides for high power vector dissipative soliton ultrafast fiber laser. *Laser Photon Rev* (2022) 16:2100255. doi:10.1002/lpor.202100255

32. Liu M, Wu H, Liu X, Wang Y, Lei M, Liu W, et al. Optical properties and applications of SnS_2 SAs with different thickness. *Opto-Electronic Adv* (2021) 4:200029. doi:10.29026/oea.2021.200029

33. Wang YW, Liu S, Zeng BW, Huang H, Xiao J, Li JB, et al. Ultraviolet saturable absorption and ultrafast carrier dynamics in ultrasmall black phosphorus quantum dots. *Nanoscale* (2017) 9:4683–90. doi:10.1039/C6NR09235G

34. Wang Y, Huang G, Mu H, Lin S, Chen J, Xiao S, et al. Ultrafast recovery time and broadband saturable absorption properties of black phosphorus suspension. *Appl Phys Lett* (2015) 107:091905. doi:10.1063/1.4930077

35. Jhon YI, Koo J, Anasori B, Seo M, Lee JH, Gogotsi Y, et al. Metallic MXene saturable absorber for femtosecond mode-locked lasers. *Adv Mater* (2017) 29:1702496. doi:10.1002/adma.201702496

36. Wang Y, Deng Z-L, Hu D, Yuan J, Ou Q, Qin F, et al. Atomically thin noble metal dichalcogenides for phase-regulated meta-optics. *Nano Lett* (2020) 20:7811–8. doi:10.1021/acs.nanolett.0c01805

37. Liu W, Liu M, Chen X, Shen T, Lei M, Guo J, et al. Ultrafast photonics of two dimensional $AuTe_2Se_{4/3}$ in fiber lasers. *Commun Phys* (2020) 3:15. doi:10.1038/s42005-020-0283-9

38. Liu W, Xiong X, Liu M, Xing X, Chen H, Ye H, et al. Bi_4Br_4-based saturable absorber with robustness at high power for ultrafast photonic device. *Appl Phys Lett* (2022) 120:053108. doi:10.1063/5.0077148

39. Zou J, Ruan Q, Zhang X, Xu B, Cai Z, Luo Z. Visible-wavelength pulsed lasers with low-dimensional saturable absorbers. *Nanophotonics* (2020) 9:2273–94. doi:10.1515/nanoph-2020-0022

40. Feng M, Zhan H. Facile preparation of transparent and dense CdS–silica gel glass nanocomposites for optical limiting applications. *Nanoscale* (2014) 6:3972–7. doi:10.1039/C3NR05424A

41. Sutherland RL. *Handbook of nonlinear optics*. 2nd ed. New York: Marcel Dekker (2003).